

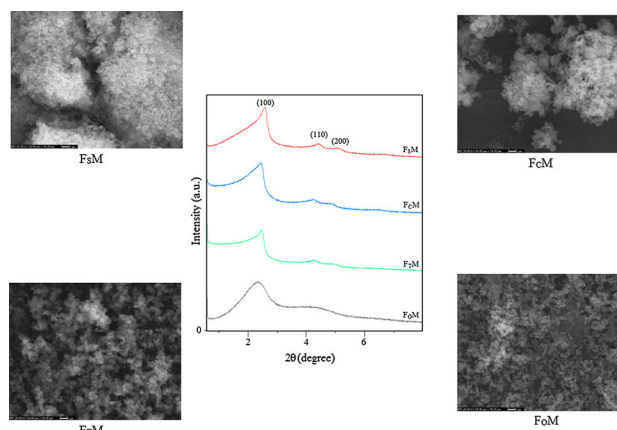
# Conversion of fly ashes from different regions to mesoporous silica: effect of the mineralogical composition

Muge Sari Yilmaz<sup>1</sup> · Nevin Karamahmut Mermer<sup>1</sup>

Received: 1 September 2015 / Accepted: 9 January 2016 / Published online: 2 February 2016  
© Springer Science+Business Media New York 2016

**Abstract** This study reports the synthesis of mesoporous MCM-41 silica materials by the hydrothermal method using five different fly ashes from the Seyitömer ( $F_S$ ), Çatalağzı ( $F_C$ ), Tunçbilek ( $F_T$ ), Orhaneli ( $F_O$ ), and Afşinelbistan ( $F_A$ ) power plants in Turkey. The mesoporous materials were not obtained from  $F_A$  which shows a lower Si/Al ratio and Si content. The synthesized MCM-41 samples from the other region fly ashes were characterized by X-ray diffraction, nitrogen adsorption–desorption, thermogravimetry, scanning electron microscopy, and high-resolution transmission electron microscopy analyses. The results demonstrated that the structural properties of the synthesized mesoporous materials were varied from depending on chemical compositions and mineral phase contents of the used fly ashes.

**Graphical Abstract** Mesoporous silica MCM-41 was synthesized from different region fly ashes in Turkey. All synthesized sample except  $F_O$ M have ordered hexagonal MCM-41 structure. Although the Si/Al ratio in the extracted solution of  $F_O$ M was high, it has low Si content. The best quality MCM-41 sample was obtained from the extracted solution of  $F_T$ M which has the highest Si/Al ratio and Si content. Taking these into account, Si/Al ratio and Si amount, and thereby mineral compositions of fly ashes play a significant role in the synthesis of mesoporous molecular sieves MCM-41.



**Keywords** MCM-41 · Fly ash · Mineral composition · Alkaline fusion

## 1 Introduction

M41S family of silicate/aluminosilicate mesoporous materials was discovered in 1992 by scientists from Mobil Oil Corporation. MCM-41 is the most well-known member and widely studied of M41S family that exhibits a hexagonal array of cylindrical mesopores [1, 2]. MCM-41 has wide fields of applications as drug delivery systems, ion exchange, adsorption, catalysis, and gas sensing [3].

MCM-41 can be synthesized in aqueous alkaline conditions using a silica source and structure-directing agents [4]. Many types of expensive silica source such as sodium silicate, tetraethyl orthosilicate (TEOS), tetramethylammonium silicate (TMA-silicate), and fumed silica are generally used for obtaining the mesoporous silica.

✉ Muge Sari Yilmaz  
mugesari@yildiz.edu.tr

<sup>1</sup> Faculty of Chemical and Metallurgical Engineering, Yıldız Technical University, Istanbul, Turkey

Development of inexpensive and environmentally acceptable ways to prepare mesoporous materials is very important [5].

Fly ash, rice husk, iron ore tailings, sepiolite, bentonite, and volclay can be transformed into MCM-41 mesoporous silica due to having high contents of silicon and aluminum that are the structural elements of MCM-41 [6–12]. Among those silica sources, the recycling of the fly ash into useful materials may have important economic and environmental implications due to generation of this waste in a large amount annually in the world.

Fly ash is produced as an industrial by-product in coal fired thermal power plants during combustion of pulverized coal and air [13, 14]. The combustion of coal forms about 37 % of the world's total electricity production [15]. This rate is more than 25 % in Turkey [16]. Huge amounts of coal fly ashes and other combustion products are generated in Turkey every year.

Fly ash is widely used for many years in a wide range of applications as a substitute for fine aggregates in cement and concrete, as filler in plastics and paints, as an adsorbent, in bricks, ceramic tiles, glass, and glass–ceramics, in the synthesis of zeolites, in road pavement and embankments, in soil amendment and stabilization, mine reclamation, etc. [13]. Although it has been used in a wide range of industries, the recycling rate of it is still low and its disposal is improper. This results in several environmental problems [14, 17].

In the literature, the conversion of coal fly ash into mesoporous silica has recently investigated [18–21]. According to these studies, it was seen that proper selection of the Si/Al ratio and Si contents in the extracted solutions of fly ashes was necessary to obtain of ordered mesoporous silica. The Si/Al ratio and Si content were related to chemical and mineralogical compositions of fly ash. Physical, chemical, mineralogical, and pozzolanic features of fly ashes show variability from region to region, even in the same region [22]. Therefore, the usages of five fly ashes from different regions in Turkey in the synthesis of MCM-41 were investigated and the structural properties of products were compared in this study. The structural

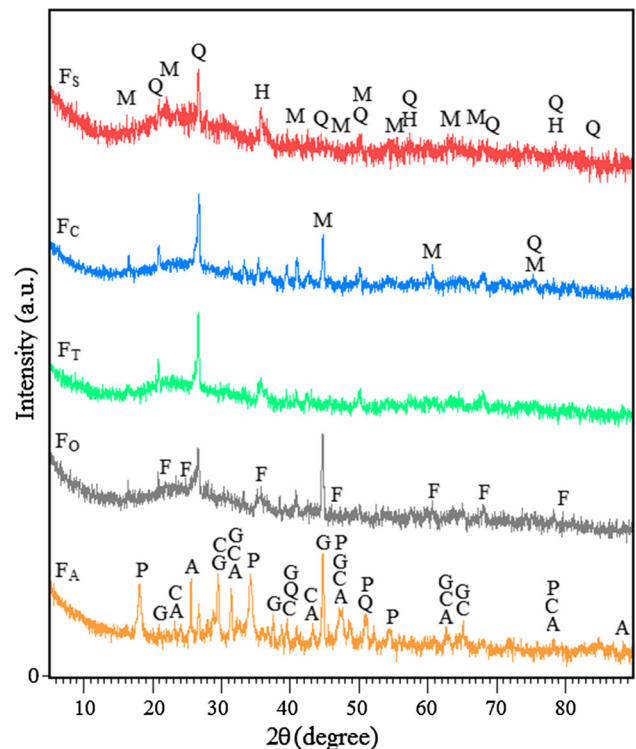


**Fig. 1** XRD patterns of fly ashes (Q: quartz, H: hematite, M: mullite, F: ferrosilite, P: portlandite, C: calcite, A: anhydrite, and G: gehlenite)

properties of the synthesized materials were characterized by some of characterization techniques.

## 2 Materials and methods

### 2.1 Materials and characterization

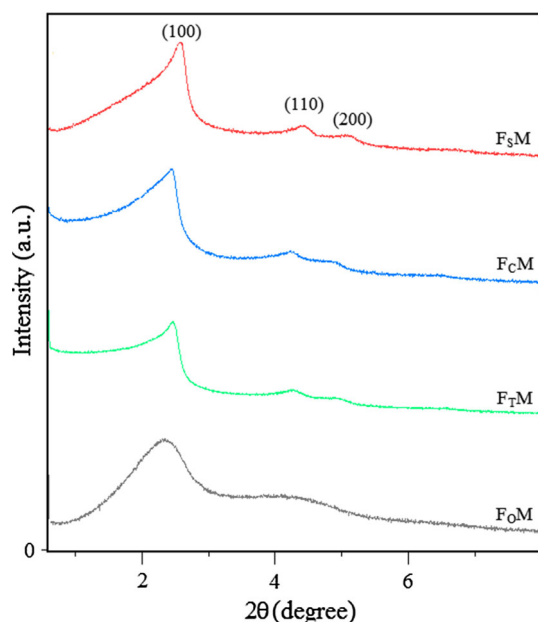
Hexadecyltrimethylammonium bromide (HDTMA-Br) as a template, sodium hydroxide (NaOH), sulfuric acid ( $H_2SO_4$ ), and deionized water were used in the MCM-41 synthesis process. The coal fly ashes were obtained from Seyitömer, Çatalağzı, Tunçbilek, Orhaneli, and Afşinelbistan thermal power stations, Turkey. Before the experimental study, fly ashes sieved on a 60-mesh standard sieve. Seyitömer, Çatalağzı, Tunçbilek, Orhaneli, and Afşinelbistan fly ashes were

**Table 1** Chemical composition of fly ashes (wt%)

Fly ash	Na <sub>2</sub> O	MgO	Al <sub>2</sub> O <sub>3</sub>	SiO <sub>2</sub>	SO <sub>3</sub>	K <sub>2</sub> O	CaO	TiO <sub>2</sub>	Fe <sub>2</sub> O <sub>3</sub>
F <sub>S</sub>	0.60	3.50	21.60	58.90	1.40	1.70	2.83	0.65	8.87
F <sub>C</sub>	0.40	2.00	28.80	57.80	0.27	3.51	0.99	1.06	5.04
F <sub>T</sub>	0.30	3.50	21.90	61.20	0.88	1.40	1.82	0.74	8.23
F <sub>O</sub>	0.40	3.20	26.50	52.50	2.10	1.99	4.22	0.60	8.51
F <sub>A</sub>	–	1.00	6.30	14.80	13.80	0.53	58.30	0.69	4.59

**Table 2** Concentrations of Si, Al, and Na in the solutions and synthesized samples

Concentrations	F <sub>S</sub> <sup>a</sup>	F <sub>S</sub> M <sup>b</sup>	F <sub>C</sub>	F <sub>C</sub> M <sup>b</sup>	F <sub>T</sub> <sup>a</sup>	F <sub>T</sub> M <sup>b</sup>	F <sub>O</sub> <sup>a</sup>	F <sub>O</sub> M <sup>b</sup>	F <sub>A</sub> <sup>a</sup>
Si	6126	283,300	8141	220,600	10,710	212,600	4745	299,550	1174
Al	346	23,260	501	21,420	390	13,270	269	30,870	1274
Na	49,320	–	57,490	–	55,120	–	48,140	–	54,020
Si/Al	17.69	12.18	16.25	10.30	27.46	16.02	17.61	9.70	0.92

<sup>a</sup> The unit of the concentrations (mg/L)<sup>b</sup> The unit of the concentrations (mg/kg)**Fig. 2** XRD patterns of the synthesized samples

denoted as F<sub>S</sub>, F<sub>C</sub>, F<sub>T</sub>, F<sub>O</sub>, and F<sub>A</sub>, respectively. The chemical analysis of the ashes was determined by X-ray fluorescence (XRF) using a PANalytical MiniPal4 spectrometer. Crystalline phases were characterized via X-ray diffraction (XRD) using an X-ray diffractometer (Philips PANalytical X'Pert-Pro) with CuK $\alpha$  radiation ( $\gamma = 1.540 \text{ \AA}$ ) at operating parameters of 40 mA and 45 kV with step size  $0.02^\circ$  over the scanning range  $2\theta = 5^\circ\text{--}90^\circ$  for fly ashes and  $2\theta = 0.58^\circ\text{--}8^\circ$  for synthesized samples.

The amounts of Si, Al, and Na in the extracted solutions and prepared samples were analyzed using Perkin-Elmer Optima 2100 DV inductively coupled plasma optical emission spectrometry (ICP-OES). Nitrogen adsorption isotherms of the synthesized samples were measured at 77 K on a Micromeritics ASAP 2020 Surface Area and Porosimetry Analyzer. Samples were degassed at 300 °C and 4 h before the analysis. Brunauer–Emmett–Teller surface areas of the synthesized samples were determined over a relative pressure ( $p/p^\circ$ ) range from 0.03 to 0.30. Pore size distributions were calculated from the adsorption branch of the isotherms using the Barrett–Joyner–Halenda

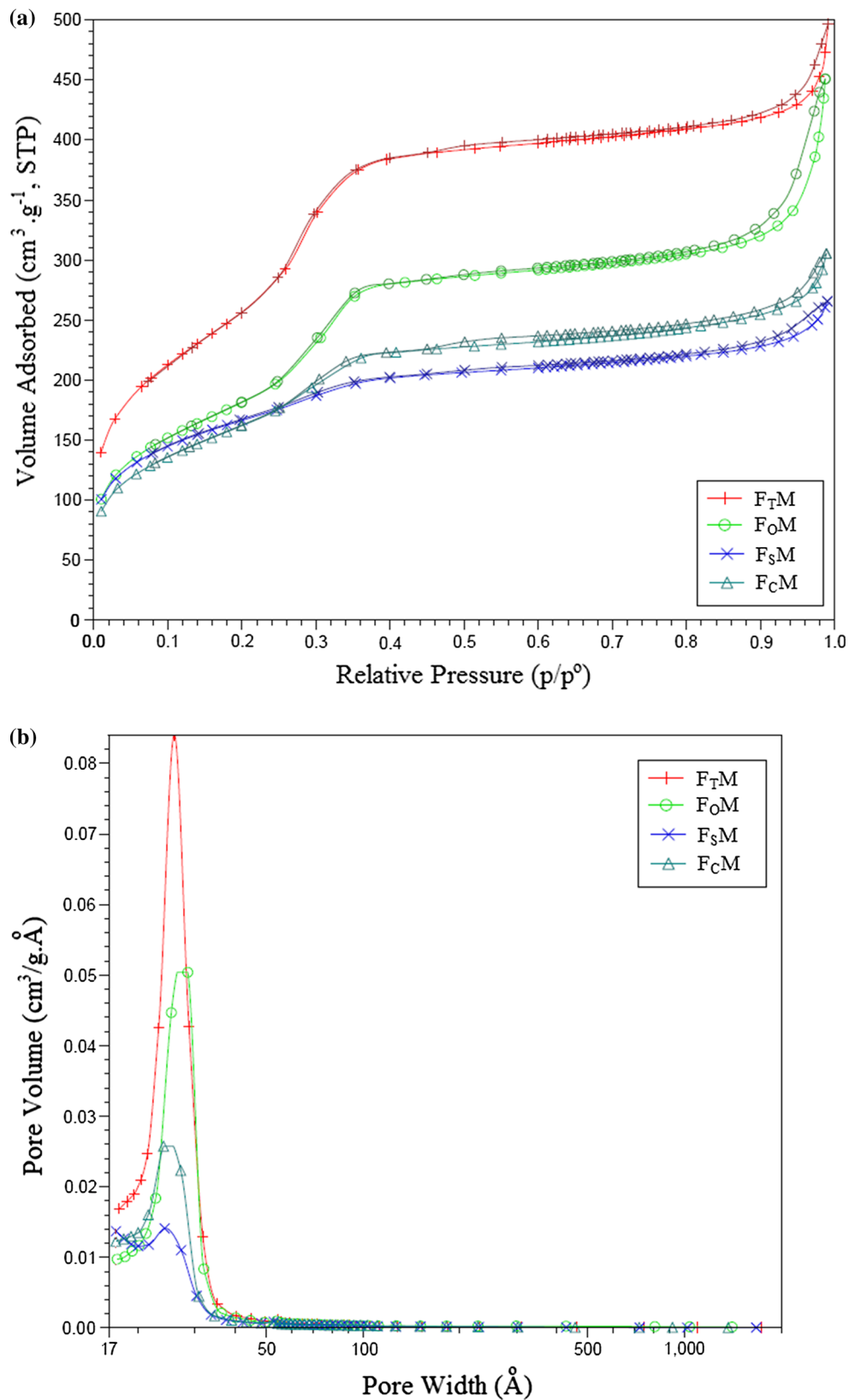
method. Thermogravimetry (TG) and derivative thermogravimetry (DTG) analyses of as-synthesized samples were carried out in a Perkin-Elmer Pyris Diamond thermal analyzer over a temperature range of 30–700 °C under nitrogen atmosphere with a rate of 200 mL/min at 15 °C/min. Scanning electron microscopy (SEM) analysis was studied by using a CamScan Apollo 300 SEM instrument. High-resolution transmission electron microscopy (HRTEM) observations were performed on JEOL-2100 HRTEM operating at 200 kV (LaB<sub>6</sub> filament).

## 2.2 Synthesis

For the synthesis of mesoporous materials, alkaline fusion process was applied to extraction of Si and Al species in the coal fly ash. The parameters of the fusion method were selected on the basis of conditions from previous studies [23, 24]. According to this method, the fly ash sample was mixed with NaOH in the weight ratio of 1:1.2 heated at 823 K for 1 h. The obtained fused mixture was cooled to room temperature and milled again. It was stirred in a shaking incubator with an appropriate amount of distilled water at room temperature for 24 h. The resultant silica solution was separated from the mixture by a filtration process. Concentrations of Si, Al, and Na in the extracted solutions were determined by ICP-OES.

In a typical synthesis of MCM-41, a given amount of HDTMA-Br was dissolved in the distilled water at room temperature. After the surfactant was completely dissolved in the water, the obtained silica solution from fusion process was added drop by drop. Resulting mixture was stirred for 1 h and pH adjusted to 11 via addition of sulfuric acid. This process results in a milky white solid precipitate formation, and it was aged at room temperature for 1 day. Then, the obtained solid was filtered, washed with deionized water, and dried at 105 °C for 12 h, and the as-synthesized sample was finally calcined at 550 °C for 6 h to remove the remaining surfactant. The samples obtained from F<sub>S</sub>, F<sub>C</sub>, F<sub>T</sub>, F<sub>O</sub>, and F<sub>A</sub> accordingly were here after labeled as F<sub>S</sub>M, F<sub>C</sub>M, F<sub>T</sub>M, F<sub>O</sub>M, and F<sub>A</sub>M, respectively. Since the synthesis yield of F<sub>A</sub>M was very low, the amount of synthesized sample was very low as well. Therefore, characterization analysis of this sample was not succeeded.

**Fig. 3** **a** N<sub>2</sub> adsorption–desorption isotherms of synthesized MCM-41 samples.  
**b** Pore size distributions



### 3 Result and discussion

#### 3.1 Properties of fly ashes and extracted solutions

The chemical compositions of the as-received coal fly ash powders are listed in Table 1. The main components of the fly ashes were silica and alumina except  $F_A$ . The highest silica and alumina contents were found in  $F_T$  and  $F_C$ , respectively, and the lowest for the  $F_A$ . Consequently, the chemical content of the ashes varies depending on the fly ash type.

The XRD patterns of fly ashes from different regions in Turkey are shown in Fig. 1. It can be revealing that the main crystalline phases found in the  $F_S$ ,  $F_C$ ,  $F_T$ , and  $F_O$  were mainly mullite and quartz and some amounts of hematite and ferrosilite. However, the XRD analysis of  $F_A$  showed that the main crystalline phases were calcite, anhydrite, portlandite, gehlenite, and quartz. These results were also confirmed by their chemical compositions analysis as shown in Table 1.

The chemical compositions of the extracted solutions which were obtained after the fusion process are listed in Table 2. It was seen from the table that the highest Si concentration was found in the extract of  $F_T$ . The Si content in the extract of  $F_T$  was significantly higher than Al.

However, the highest Al concentration was found in the extract of  $F_A$ , and it has the lowest Si amount. In addition, the Si/Al ratio of  $F_A$  is much lower than of the other fly ashes. The difference in Si/Al extracted amounts was due to the different mineral phase contents of fly ashes.

#### 3.2 Characterization of synthesized MCM-41 samples

XRD patterns of the synthesized samples except  $F_A M$  are shown in Fig. 2. The XRD analysis of  $F_A M$  was not succeeded since there was not enough amount of this sample. This can be related to the extracted solution of  $F_A$  having very low Si/Al molar ratio and Si content. The XRD patterns exhibited (100), (110), and (200) reflections which are characteristics of the MCM-41 structure [4], could be observed for  $F_S M$ ,  $F_C M$ , and  $F_T M$ .  $F_O M$  has non-ordered hexagonal MCM-41 structure due to disappearing of (200) peak. Although the Si/Al content of the extracted solution of  $F_O$  was high compared to  $F_C$ ,  $F_O M$  presents a worse crystallinity compared to  $F_C M$ . This may be attributed to low concentration of Si in the extracted solution of  $F_O$ . According to analysis results, it was determined that the quality of the synthesized MCM-41 was depending on the Si/Al ratio and Si content in the extracted solution.

The chemical compositions of the synthesized samples are listed in Table 2. It was seen that Si/Al ratios in the

synthesized samples were lower than Si/Al ratio in the extracted solutions. In contrast, Majchrzak-Kuceba and Nowak found Si/Al ratio of mesoporous materials produced from fly ash higher than the Si/Al in the filtrates [6]. The highest Si/Al ratio in the synthesized samples was found as 16.02 in the  $F_T M$ . Chang et al. [25] showed that MCM-41 from fly ash can be synthesized with a Si/Al = 13.4. In this study, it was observed that highly ordered MCM-41 with a Si/Al = 10.30 and even non-ordered MCM-41 with a Si/Al = 9.70 were successfully synthesized.

Figure 3 shows the  $N_2$  adsorption–desorption isotherms and pore size distribution curves of synthesized MCM-41 samples. All samples exhibited a typical type IV with a H1 hysteresis loop according to the IUPAC classification, showing the mesoporous nature of the solids. A well-defined steps at high relative pressures ( $p/p^\circ = 0.45–1.0$ ) indicate that the samples have narrow pore size distributions and the pore size is nearly uniform. The BET surface area and pore volume of synthesized samples vary from 577.99 to 1048.54 and 0.37 to 0.66  $cm^3/g$ , respectively, as listed in Table 3. It can be seen that  $F_T M$  has the highest BET surface area (1048.54  $m^2/g$ ) and pore volume (0.66  $cm^3/g$ ). This BET value of  $F_T M$  was very high according to any sample prepared from fly ash in the literature as follows: 383  $m^2/g$  [23], 610  $m^2/g$  [6], 732  $m^2/g$  [20], 735  $m^2/g$  [25], 740  $m^2/g$  [7], and 842  $m^2/g$  [18]. Previously, Halina et al. [7] showed that the pore size of MCM-41 synthesized from coal fly ash was 2.3 nm. The pore size distribution of the  $F_T M$  determined by the adsorption branch of the isotherm using BJH method reveals a one sharp peak at about 3.14 nm. Compared with the synthesized MCM-41 samples from the other fly ashes, the pore size distribution of  $F_T M$  is narrower and the average size is much lower.

The results of TG/DTG analysis of as-synthesized MCM-41 samples are shown in Fig. 4a, b. Three main stages of weight loss were observed on the TG/DTG curves of the all samples. The first weight loss was attributed to the removal of physisorbed water

**Table 3** Textural properties of the synthesized samples

Sample name	$S_{BET}^a$ ( $m^2/g$ )	$d_{BJH}^b$ (nm)	$V_p^c$ ( $cm^3/g$ )
$F_S M$	577.99	3.41	0.3655
$F_C M$	606.90	3.37	0.4106
$F_T M$	1048.54	3.14	0.6642
$F_O M$	715.55	3.97	0.5274
$F_A M$	n.m.	n.m.	n.m.

n.m. not measured

<sup>a</sup> Specific surface area

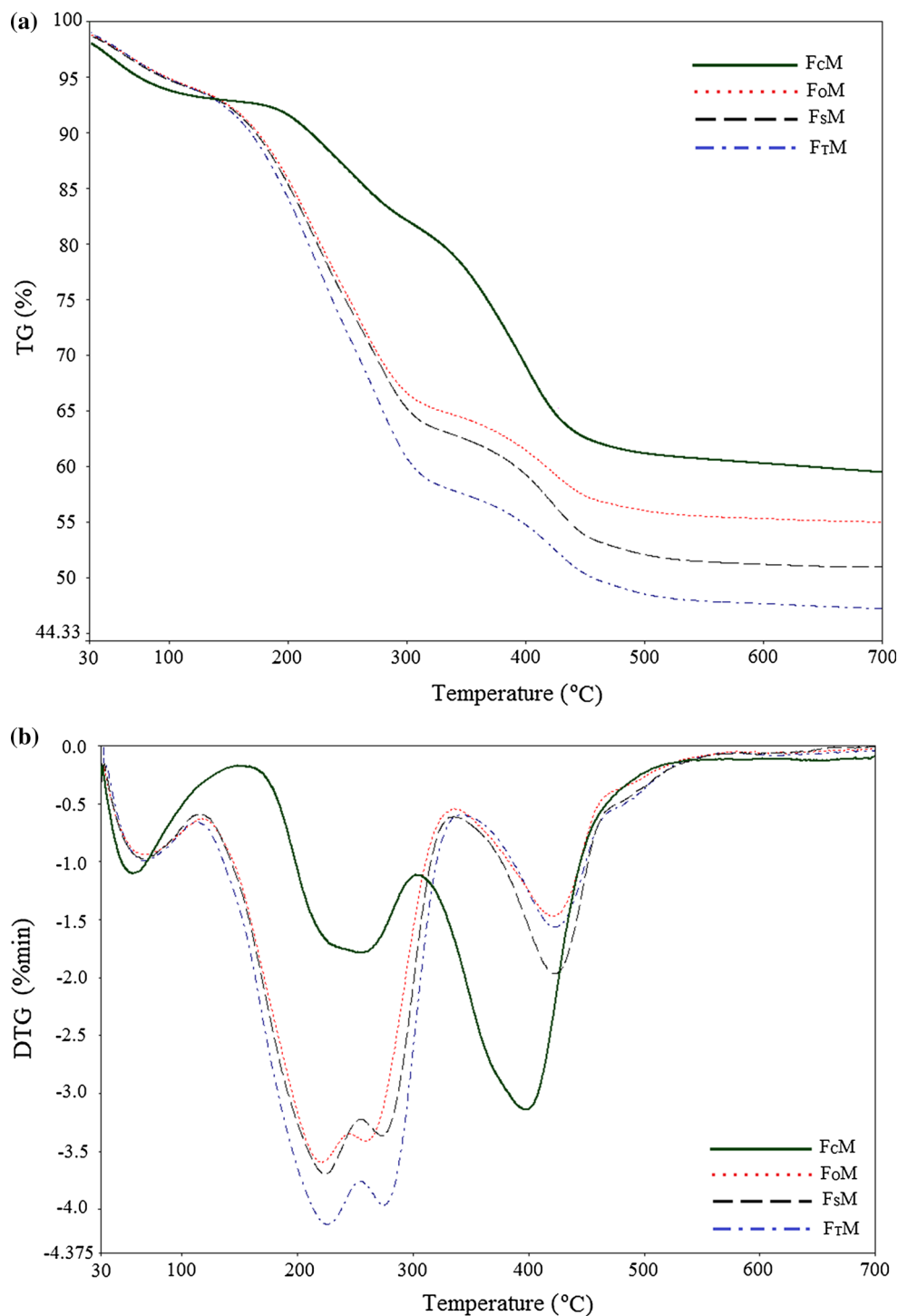
<sup>b</sup> Pore diameter calculated by BJH theory

<sup>c</sup> Total pore volume

molecules. The second weight loss corresponds to the decomposition of template appeared as two partly overlapping peaks on the DTG curves of F<sub>O</sub>M, F<sub>S</sub>M, and F<sub>T</sub>M except F<sub>C</sub>M. The final step was related to the decomposition of remaining template and condensation

of silanol groups [26]. The individual values of weight loss and temperature range for all the samples are listed in Table 4. The total weight loss of F<sub>C</sub>M was found as 38.52 %, and this weight loss was lower than the weight loss of the other samples. It can be observed that the

**Fig. 4** TG/DTG curves of as-synthesized MCM-41 samples

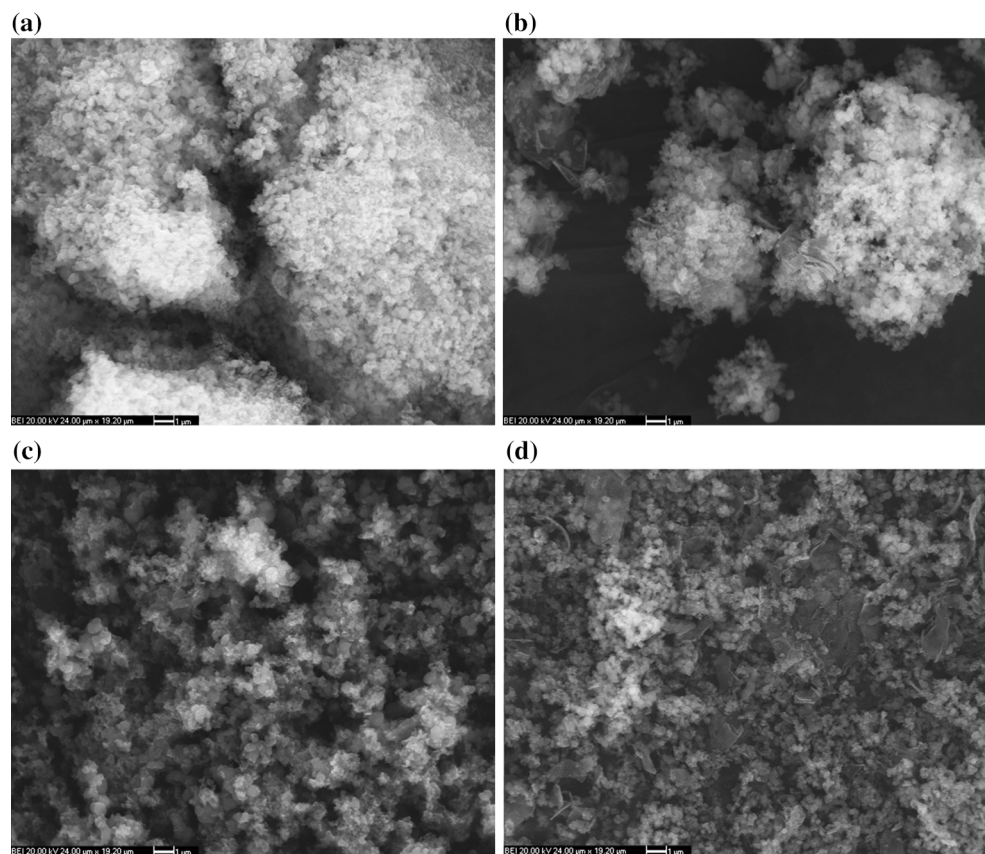


**Table 4** Weight losses and temperature range for all the synthesized samples

Samples	Reaction stages	Temperature range (°C)	Weight loss (%)
F <sub>S</sub> M	First	30–115	5.85
	Second	115–335	31.13
	Final	335–648	11.95
F <sub>C</sub> M	First	30–134	5.43
	Second	134–305	11.21
	Final	305–646	21.89
F <sub>T</sub> M	First	32–114	5.77
	Second	114–342	36.46
	Final	342–647	10.31
F <sub>O</sub> M	First	30–118	5.66
	Second	118–337	29.40
	Final	337–646	9.57

thermal behavior of F<sub>S</sub>M, F<sub>T</sub>M, and F<sub>O</sub>M was similar to each other, while F<sub>C</sub>M was different.

Representative SEM images of MCM-41 samples synthesized from different fly ashes are shown in Fig. 5. The all samples have hexagonal-shaped agglomerated particles with a size below of 1 μm. This result was close to the result obtained by Halina et al. [7] for MCM-41 synthesized from coal fly ash. HRTEM micrographs of synthesized MCM-41 samples are shown in Fig. 6. Figure 6 shows the well-ordered hexagonal arrays of uniform channels. The pore size of the samples was determined as approximately 3.25 nm for F<sub>S</sub>M, 3.1 nm for F<sub>C</sub>M, and 3 nm for F<sub>T</sub>M, consistent with the result of N<sub>2</sub> adsorption–desorption analysis. On the other hand, the pore size of F<sub>O</sub>M could not be determined since it has distorted pore ordering as shown in Fig. 6d.

**Fig. 5** SEM images of **a** F<sub>S</sub>M, **b** F<sub>C</sub>M, **c** F<sub>T</sub>M, and **d** F<sub>O</sub>M

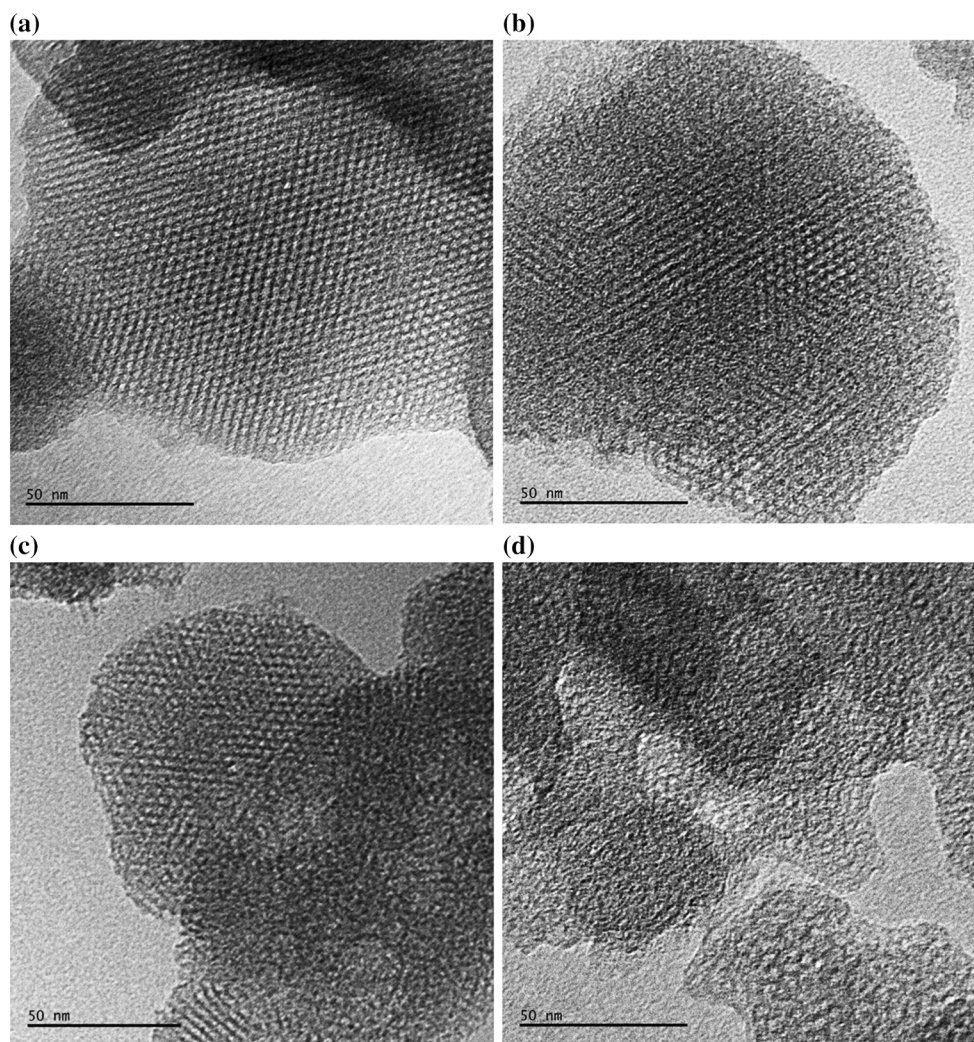


**Fig. 6** HRTEM micrographs of synthesized samples **a**  $F_S M$ , **b**  $F_C M$ , **c**  $F_T M$ , and **d**  $F_O M$

#### 4 Conclusions

Mesoporous silica MCM-41 was synthesized from different region fly ashes in Turkey except Afsin–Elbistan region fly ash due to its low Si/Al ratio and Si content. All synthesized MCM-41 samples except the sample synthesized from the extracted solution of Orhaneli fly ash have ordered hexagonal MCM-41 structure. Although the Si/Al ratio in the extracted solution of Orhaneli fly ash was high, it has low Si content. The best quality MCM-41 sample was obtained from the extracted solution of Tunçbilek fly ash which has the highest Si/Al ratio and Si content. Taking these into account, it was seen that Si/Al ratio and Si amount, and thereby mineral compositions of fly ashes play a significant role in the synthesis of mesoporous molecular sieves MCM-41. The present study has provided a useful method on conversion of fly ash into a mesoporous molecular sieve, which resulted in the elimination of the disposal problem of it.

**Acknowledgments** We gratefully acknowledge the financial support provided by the Research Found of Yıldız Technical University. Project Number: 2014-07-01-GEP03. We also thank to Neslihan Şener for experimental assistance.

#### References

1. Zhao XS, Lu GQM, Millar GJ (1996) Advances in mesoporous molecular sieve MCM-41. *Ind Eng Chem Res* 35(7):2075–2090. doi:[10.1021/ie950702a](https://doi.org/10.1021/ie950702a)
2. Kruk M, Jaroniec M, Sayari A (1997) Application of large pore MCM-41 molecular sieves to improve pore size analysis using nitrogen adsorption measurements. *Langmuir* 13(23):6267–6273. doi:[10.1021/la970776m](https://doi.org/10.1021/la970776m)
3. Vallet-Regi M, Ramila A, Del Real R, Pérez-Pariente J (2001) A new property of MCM-41: drug delivery system. *Chem Mater* 13(2):308–311
4. Kresge C, Leonowicz M, Roth W, Vartuli J, Beck J (1992) Ordered mesoporous molecular sieves synthesized by a liquid-crystal template mechanism. *Nature* 359(6397):710–712
5. Karandikar P, Patil K, Mitra A, Kakade B, Chandwadkar A (2007) Synthesis and characterization of mesoporous carbon



- through inexpensive mesoporous silica as template. *Microporous Mesoporous Mater* 98(1):189–199
6. Majchrzak-Kuceba I, Nowak W (2011) Characterization of MCM-41 mesoporous materials derived from polish fly ashes. *Int J Miner Process* 101(1):100–111
  7. Halina M, Ramesh S, Yarmo M, Kamarudin R (2007) Non-hydrothermal synthesis of mesoporous materials using sodium silicate from coal fly ash. *Mater Chem Phys* 101(2):344–351
  8. Braga RM, Barros JM, Melo DM, Melo MA, Aquino FdM, Freitas JcO, Santiago RC (2013) Kinetic study of template removal of MCM-41 derived from rice husk ash. *J Therm Anal Calorim* 111(2):1013–1018
  9. Yu H, Xue X, Huang D (2009) Synthesis of mesoporous silica materials (MCM-41) from iron ore tailings. *Mater Res Bull* 44(11):2112–2115
  10. Jin S, Qiu G, Xiao F, Chang Y, Wan C, Yang M (2007) Investigation of the structural characterization of mesoporous molecular sieves MCM-41 from sepiolite. *J Am Ceram Soc* 90(3):957–961
  11. Ali-Dahmane T, Adjdir M, Hamacha R, Villieras F, Bengueddach A, Weidler PG (2014) The synthesis of MCM-41 nanomaterial from Algerian Bentonite: the effect of the mineral phase contents of clay on the structure properties of MCM-41. *C R Chim* 17(1):1–6
  12. Adjdir M, Ali-Dahmane T, Friedrich F, Scherer T, Weidler P (2009) The synthesis of Al-MCM-41 from volclay: a low-cost Al and Si source. *Appl Clay Sci* 46(2):185–189
  13. Blissett R, Rowson N (2012) A review of the multi-component utilisation of coal fly ash. *Fuel* 97:1–23
  14. Ahmaruzzaman M (2010) A review on the utilization of fly ash. *Prog Energy Combust Sci* 36(3):327–363
  15. Zevenbergen C, Bradley JP, Van Reeuwijk LP, Shyam A, Hjelmar O, Comans RN (1999) Clay formation and metal fixation during weathering of coal fly ash. *Environ Sci Technol* 33(19):3405–3409
  16. Republic of Turkey MoEaNR (2013)
  17. Querol X, Moreno N, Umana J, Alastuey A, Hernández E, Lopez-Soler A, Plana F (2002) Synthesis of zeolites from coal fly ash: an overview. *Int J Coal Geol* 50(1):413–423
  18. Kumar P, Mal N, Oumi Y, Yamana K, Sano T (2001) Mesoporous materials prepared using coal fly ash as the silicon and aluminium source. *J Mater Chem* 11(12):3285–3290
  19. Chandrasekar G, You K-S, Ahn J-W, Ahn W-S (2008) Synthesis of hexagonal and cubic mesoporous silica using power plant bottom ash. *Microporous Mesoporous Mater* 111(1):455–462
  20. Misran H, Singh R, Begum S, Yarmo MA (2007) Processing of mesoporous silica materials (MCM-41) from coal fly ash. *J Mater Process Technol* 186(1):8–13
  21. Hui K, Chao C (2006) Synthesis of MCM-41 from coal fly ash by a green approach: influence of synthesis pH. *J Hazard Mater* 137(2):1135–1148
  22. Güler GGE, İpekoğlu Ü, Mordoğan H (2005) Uçucu Küllerin Özellikleri ve Kullanım Alanları
  23. Ojha K, Pradhan NC, Samanta AN (2004) Zeolite from fly ash: synthesis and characterization. *Bull Mater Sci* 27(6):555–564
  24. Shigemoto N, Hayashi H, Miyaura K (1993) Selective formation of Na-X zeolite from coal fly ash by fusion with sodium hydroxide prior to hydrothermal reaction. *J Mater Sci* 28(17):4781–4786
  25. Chang H-L, Chun C-M, Aksay IA, Shih W-H (1999) Conversion of fly ash into mesoporous aluminosilicate. *Ind Eng Chem Res* 38(3):973–977
  26. Souza M, Silva A, Aquino J, Fernandes V, Araújo A (2004) Kinetic study of template removal of MCM-41 nanostructured material. *J Therm Anal Calorim* 75(2):693–698